COBEM 2021 26th International Congress of Mechanical Engineering
November 22-26, 2021, Virtual Congress, Brazil

COB-2021-0745
THE INFLUENCE OF PRINTING PARAMETERS ON MONOLAYER PART FEATURES IN FUSED FILAMENT FABRICATION

Thiago Glissoi Lopes
São Paulo State University, Av. Eng Edmundo C. Coube, 14-01 - Núcleo Hab. Pres. Geisel, Bauru – SP, 17033-360
thiago.glissoi@unesp.br

Laura Marques Queiroz
Industrial Technical College "Prof. Isaac Portal Roldán", Av. Nações Unidas, 58-50 - Nucleo Res. Pres. Geisel, Bauru - SP, 17033-260
laura.marques@unesp.br

Verena Soares Bombonatti
Campinas State University, Cidade Universitária Zeferino Vaz – Barão Geraldo, Campinas – SP, 13083-970
v177036@dac.unicamp.br

Matheus Godoy Fonseca do Carmo
São Paulo State University, Av. Eng Edmundo C. Coube, 14-01 - Núcleo Hab. Pres. Geisel, Bauru – SP, 17033-360
matheusgodoyfcarmo@gmail.com

Paulo Roberto de Aguiar
São Paulo State University, Av. Eng Edmundo C. Coube, 14-01 - Núcleo Hab. Pres. Geisel, Bauru – SP, 17033-360
paulo.aguiar@unesp.br

Thiago Valle França
São Paulo State University, Av. Eng Edmundo C. Coube, 14-01 - Núcleo Hab. Pres. Geisel, Bauru – SP, 17033-360
thiago.franca@unesp.br

Abstract. *The Fused Filament Fabrication (FFF) process deals with the manufacturing of parts by means of the addition of material in successive layers. The monitoring of additive manufacturing processes, such as the FFF, has been the subject of various studies. The FFF process has a critical point in its beginning, during the fabrication of the first layer. If defects are detected at this point, the FFF process can be interrupted, thus, preventing wastessuch as raw material, machine time, energy, premature maintenance due to machine wear, and others. The quality of parts obtained by FFF are directly influenced by the printing parameters, determined by the process operator in order to achieve, for example, a certain stress resistance, surface roughness, or to correct minor calibration variations in the 3D printer mechanical elements. It is a common practice in FFF monitoring studies to print what is called a monolayer part, which is the fabrication either of a part that consists of a single layer, or of just the first layer of a multilayered part. Visual inspection of parts for quality assessment is a very common practice in monitoring studies, due to its capability of easily detecting countless geometric variations on a certain part. Thus, the present work sought to study, by means of visual inspection, the influence of several printing parameters upon the geometry and surface quality of monolayer parts obtained by the FFF process. In order to facilitate the visual inspection of the parts, a scanner was used to digitalize the upper surface of each printed part. The results showed that each printing parameter has an influence on the quality of the obtained parts. And that influence can result in defects that range from minor superficial deviations to major superficial and geometric ones.*

Keywords: *Fused Filament Fabrication, Process Monitoring, Printing Parameters, Part Evaluation, Visual Inspection*

1. INTRODUCTION

Additive manufacturing (AM) is a category of manufacturing processes that are based on the successive addition of material, usually in the form of layers, in order to fabricate, starting from raw material, a desired part (ISO/ASTM, 2015; VOLPATO, 2017). Examples of processes that are part of the AM category are the Stereolithography (SLA), Selective Laser Sintering (SLS), and Directed Energy Deposition (DED). Among the processes held in the AM category, one of the most popular and widespread is the Fused Filament Fabrication (FFF) process (LOPES *et al.*, 2018; SINGH; RAMAKRISHNA; SINGH, 2017). The FFF widespread popularity is justified because it is an affordable process and due to the simplicity of the necessary manufacturing machinery compared to other AM processes

(BOSCHETTO & BOTTINI, 2015). In the FFF process, a filament, usually made of polymeric material, is extruded through a nozzle, mounted on a movable extruder head, and deposited on a table or on top of a previous layer in the shape of tracks. The tracks are responsible for filling the pattern adopted for each layer of the part (VOLPATO, 2017).

The FFF process usually uses polymeric filament such as Acrylonitrile Butadiene Styrene (ABS), Polyethylene Terephthalate (PET), Polyether Ether Ketone (PEEK), Nylon, Polyamide, and Polycarbonate as raw material (VOLPATO, 2017). Among these materials, the Polylactic Acid (PLA) stands out for its lower printing temperature compared to other polymers, and for presenting non-toxicity, biocompatibility, and biodegradability characteristics; and the Polyethylene Terephthalate Glycol (PETG), for its intermediate characteristics between PLA and ABS, being more ductile, flexible and tenacious than PLA, and easier to handle than ABS (LIU; LEI; XING, 2019; LIU et al., 2019; SANTANA et al., 2018).

The adoption of AM processes has been growing in recent years, establishing itself as an alternative to traditional subtractive and forming manufacturing methods (LOPES *et al.*, 2018). As an example, it is possible to observe the study by the consultancy agency Wohlers Associates, in which the results presented show that the share of the invoicing of parts for industry in the global AM market jumped from 3.9% in 2003 to 35% in 2013 (OETTMEIER; HOFMANN, 2017). Another survey, carried out by the company Sculpteo, a provider of 3D printing services, revealed that FFF was the most used AM process among the companies consulted, with an adoption of 46% in 2018, a percentage that grows to 75% when considering only the businesses that own any AM equipment, followed by SLS with 38% and SLA with 34% (SCULPTEO, 2020). These examples demonstrate how the AM market is booming and the importance, in this scenario, of the FFF process.

For practices intended at monitoring the FFF process, the analysis of the first layer is an interesting approach of studying the general behavior of the part's manufacture, as well as to detect possible defects produced under certain conditions. This occurs because, as the largest basic element produced in the FFF process, as well as in other AM processes, the first layer allows for a good initial assessment of several characteristics of the complete part (WENDT *et al.*, 2016). For practices aimed at studying defects and the consequences of alterations, such as changing printing parameters, the first layer is also of special importance, as it supports the other layers necessary for the production of the piece. So, a problem of any nature in the first layer would end up significantly impacting the part (WU; YU e WANG, 2019).

The manufacturing of a part can be divided into the following steps: obtaining a 3D model of the part, slicing and printing (KOCISKO *et al.*, 2017). Obtaining a 3D model of the part can be performed by modeling the part in the desired shape and dimensions in a Computer Aided Design (CAD) software (DA SILVA, 2007). After that, the 3D model is converted to the Stereolithography File Format (STL), which describes the position of the vertices of the triangles that constitute the model. Finally, the STL file goes through the slicing step. Slicing is the stage where the 3D model is divided into layers, and in which the filling strategy is defined. It is also at this stage that several of the printing parameters, such as layers thickness and infill density, are chosen. Careful consideration of the values chosen for the different printing parameters is essential, so that the outcome is as desired (CARMO *et al.*, 2020; LOPES *et al.*, 2020).

There are several printing parameters to be defined during the slicing step (DAWOUD; TAHA; EBEID, 2016). The incorrect definition of a certain printing parameter can have a negative effect on the quality of the product obtained (LOPES *et al.*, 2020). The layer thickness defines the dimension on the Z axis of each deposited layer. A thicker layer reduces the total printing time but can compromise geometric fidelity. The filling pattern is responsible for the way in which the tracks are deposited to fill the interior of the part. There is a great variety of infill patterns to choose from, such as the concentric, linear, and honeycomb patterns. Each filling pattern presents a different behavior in terms of strength, stiffness, and stress concentration, and its parameters can also be affected by the geometry of the part/layer, which makes choosing the "ideal" pattern a complex task. The infill density printing parameter specifies how much of the internal volume is actually filled. A higher filling density results in a more resistant and rigid part, while increasing the weight and the time needed for printing(RODRÍGUEZ-PANES; CLAVER; CAMACHO, 2018).

Among the methods used to evaluate and inspect parts made using the FFF process can be cited tensile and compression tests, profilometry and microscopy, as well as less common ones, such as ultrasonic and acoustic emission. Despite being more commonly used for maintenance purposes, such as inspection of airplanes and railways, visual inspection is a resource used, also, in several fabrication fields to evaluate parts and products in search for anomalies that could indicate serious failures or defects (GE *et al.*, 2020; NAKAJIMA *et al.*, 2019; ZHANG *et al.*, 2021). Visual inspection methods are used, for example, to detect abnormalities in porosity and inclusions on parts obtained by casting (VOELKER, 2016). Other areas where visual inspection can be used include the injection of polymeric parts, to identify possible defects due to the lack of material injection, and the manufacture of bottles by the blow molding process, where relatively small deviations in shape can compromise the product usability (WU, Y. *et al.*, 2019). All of these applications illustrate that visual inspection can be an interesting and efficient way to assess the quality of the parts produced.

Due to the lack of literature regarding the evaluation of FFF monolayer parts superficial quality by means of visual inspection, the present work sought to study, by means of visual inspection, the influence of several printing parameters upon the geometry and superficial quality of monolayer parts obtained by the FFF process.

2. MATERIALS AND METHODS

2.1 Experimental procedures

The print tests were conducted on a Graber i3 model 3D printer, manufactured by GTMax3D®. This printer model includes a MK2B Dual Power PCB printing table in contact with a thermistor type temperature sensor model NTC, which is located directly in contact with a 200 x 200 x 3 mm glass surface. The Graber i3 also contains a Hotend Allmetal GTMax 3D model extruder, which has a nozzle diameter of 0.4 mm. This printer model, according to the manufacturer, is capable of achieve a printing resolution of ±0.05 mm, in X-Y and Z axis. The PLA filament utilized in the tests were manufactured by 3D Fila®. The print tests were controlled and supervised via a computer running the Repetier-Host® software. The connection between the computer and the 3D printer was made via a USB connection.

In order to identify the influence of different printing parameters on the surface quality of parts obtained by the FFF process, printing tests with the adoption of different values for selected printing parameters in the slicing stage were conducted with both PLA and PETG filaments. Even though some selected parameters by logic would not cause direct influence on the first layer printing, as the first layer printing speed parameter, those were also altered in some tests in order to confirm that statement, and also to look for indirect influence of those parameters on the overall printing process. Forced cooling was not applied on the fabrication of the monolayer parts.

The digital model of the monolayer part was modeled in the SketchUp® software. Figure 1 shows the monolayer part model adopted for the printing tests. As can be seen in Figure 1, the shape adopted is similar to that of a slice of pizza, with a width of 7 cm, length of 5 cm, and thickness of 0.3 mm, and two distinct filling patterns. The first pattern, which consists of the outer region of the part, is fabricated by means of contour lines. In sequence, the second pattern, the internal region of the part, is fabricated by means of raster lines with a raster angle of 0º.

The slicing step was conducted in the Slic3r® software, running as part of the Repetier-Host® software. Regarding the different printing parameters adopted for each test, the standard values defined by the Slic3r software for each type of raw material with 1.75 mm in diameter, G-code flavor RepRap (Marlin/Sprinter) and Graber i3 printer definitions were considered as baseline.

In each conducted test, for both 3D printing with PLA and PETG filaments, an attempt was made to alter, at least, one printing parameter at a time. Table 1 presents the parameter values adopted for each test, in addition to the indications provided by the Repetier-Host program regarding filament consumption, in millimeters, and the expected printing time, in minutes and seconds.

As the predicted filament consumption and printing time are defined as a result of the adoption of other printing parameters during the slicing step and are provided to the process operator before the printing step of the FFF process is conducted, these were depicted in this work as adopted printing parameters.

In the printing parameters listed in Table 1, the “X” indicates a printing parameter that was absent in that part. For the printing parameters required for slicing that are not shown in Table 1, the default values of the Slic3r® software were adopted.

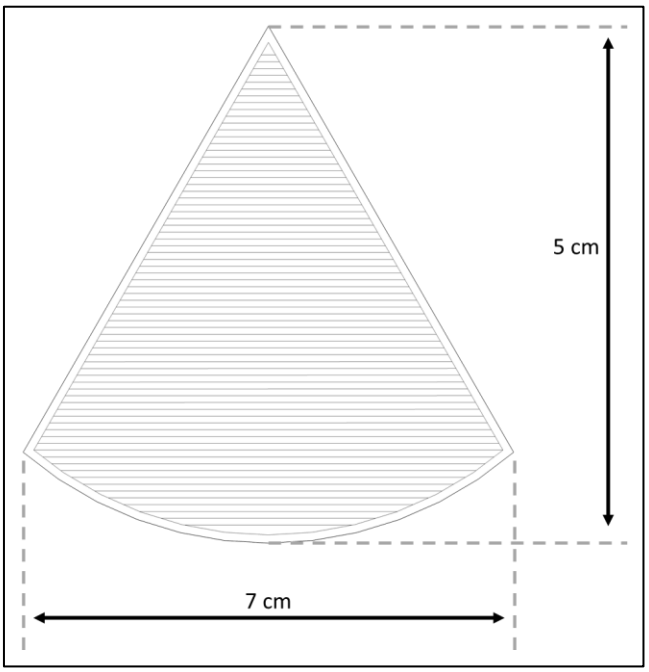

Figure 1. Workpiece model

Table 1. Adopted printing parameters.

Material		PLA										PETG			
Test nº		1	2	3	4	5	6	7	8	9	10	1	2	3	4
Consumed filament (mm)		194			212	227	223	227				194		227	227
Printing time (m:s)		4:27	4:46	3:45	5	5:03						4:27	4:46	5:03	
Skirt (nº)		1			3	2						1		2	
Brim (mm)		X				2 x 1						X		2 x 1	
Top solid printing speed (mm/s)		15		30	15										
Printing pattern		Rectilinear					Hilbert curve	Rectilinear							
Skirt distance to piece (mm)		6													
Solid printing speed (mm/s)		20													
Gaps printing speed (mm/s)		20													
Filament diameter (mm)		1.75													
First layer	Layer height (mm)	0.3													
	Infill percentage (%)	75													
	Printing speed (mm/s)	30	20									30	20		
	Extruder temperature (ºC)	205					190	212	205			245			
	Table temperature (ºC)	65							35	80		75			40

2.2 Visual inspection procedures

With the purpose of visual inspection of the parts, a DCP-L2540DW model scanner, manufactured by Brother®, was used to digitalize the upper surface of all workpieces. The printed workpieces were temporarily attached to a graph paper before digitization, in order to allow for a pixel-to-millimeter reference. The images were generated with a 400 x 400 dpi resolution and saved as a900 x 900 pixel PNG file.

With the digitized images, the visual inspection process was conducted with the aid of the Paint 3D® and PowerPoint® softwares, respectively. Firstly, the dimensional aspects were observed in the form of total width and length at the medium point of the workpieces, evaluated by means of the Paint 3D software. In sequence, their superficial anomalies were evaluated by means of highlighting punctual defective regions in the PowerPoint® software, which could indicate improper selection of certain printing parameters in the slicing step.

3. RESULTS AND DISCUSSION

3.1 Dimensional variation

Regarding the results obtained from the dimensional variation assessment, due to the quantity of conducted tests, examples of the assessment performed on PLA and PETG workpieces are presented in figure format. The remaining results are presented further in the article in table format. Also, due to the quantity of conducted tests, only instances with major dimensional variations will be further discussed with the aid of a figure representation. The authors want to specify that the in the case that brim was printed, it was removed before the digitalization of the workpieces.

In Figure 2 it is possible to observe the total width and length evaluated from PLA and PETG printed workpieces in number of pixels (px), and the pixel-to-millimeter reference established in the graph paper from Figure 2(a). This reference value was utilized to convert the sizes from pixel to millimeter for all workpieces.

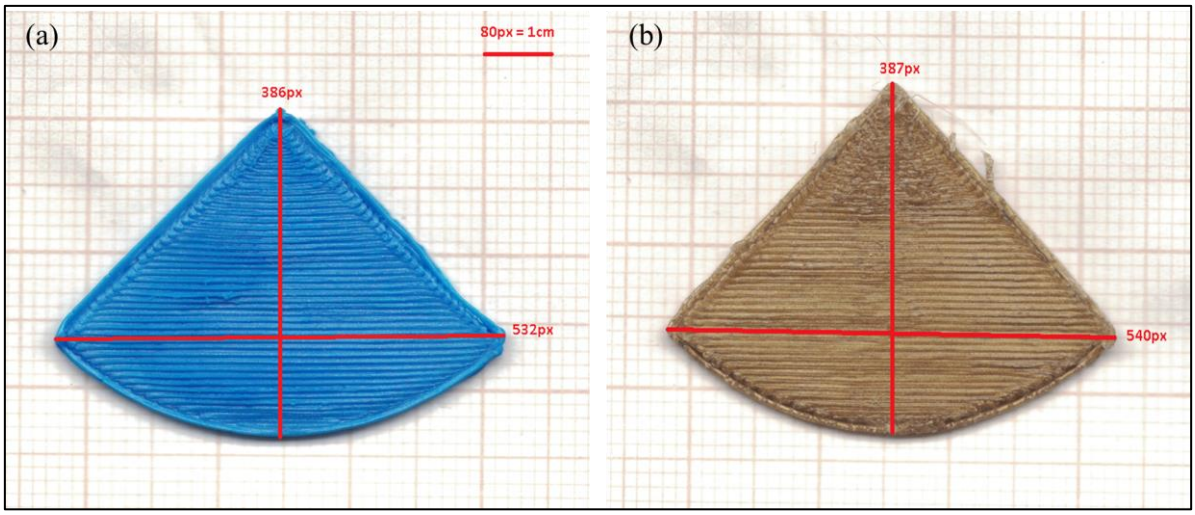

Figure 2. Workpiece dimensional variation evaluation. (a) 10ºth PLA test, (b) 3ºrd PETG test

The geometrical data evaluated are displayed in Figure 3 in order to facilitate understanding and comparison between tests. The first result that can be perceived from Figure 3 is that none of the workpieces presented the geometrical values originally defined in the proposed 3D Model, even when considering the ±0.05 mm printing resolution achievable by the Graber i3.

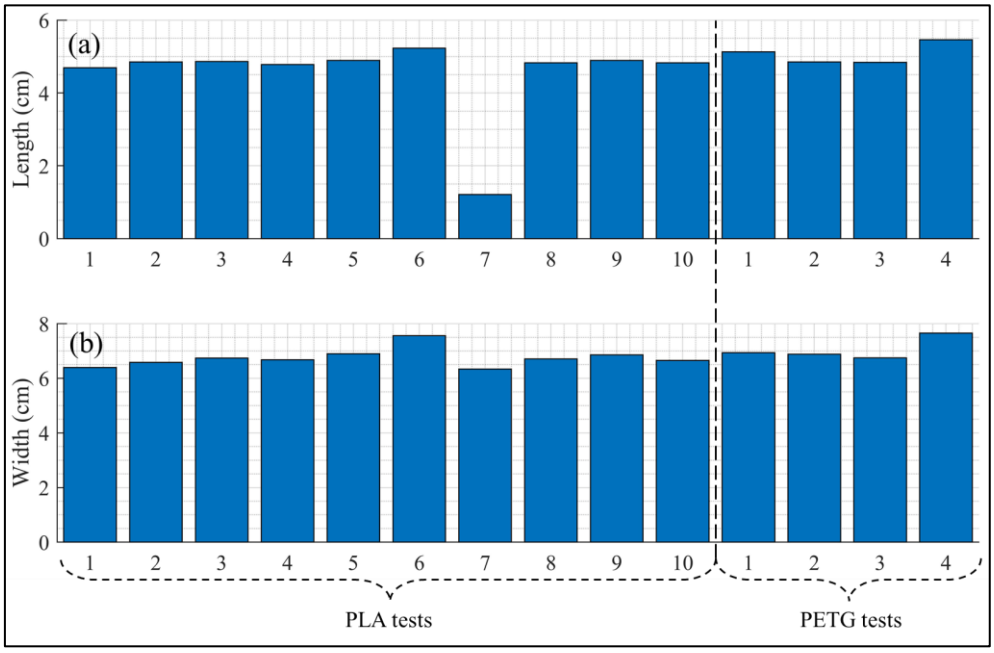

Figure 3. Evaluated workpiece dimensions in centimeters. (a) Length, (b) Width

Regarding the variations between the workpieces actual dimensions and the ones originally defined for the 3D Model, it is also possible to observe that in the majority of tests, the obtained part is smaller than the 3D model. This behavior changes only in the 6ºth PLA test, and in the 1ºst and 4ºth PETG tests. The variation in the 6ºth PLA test can be attributed to the infill pattern, that for this test was changed to Hilbert curve, as shown in Figure 4. Regarding the 1ºst PETG test, the feature that presented the higher variation in comparison to the 3D model was the total/medium point length of the workpiece, and that can be attributed to the first layer printing speed, which had a higher value than the subsequent PETG tests. Lastly, the variation in the 4ºth PETG test can be attributed to the first layer table temperature, which was lower in comparison to the preceding PETG tests. The lower table temperature caused a failure in the skirt adhesion to the printing table, which then fused with the workpiece, causing higher values than originally defined in the 3D Model.

The difference between PLA and PETG printed workpieces is notable when examining the evaluated dimensional averages. The workpiece dimensions evaluated from PETG tests showed higher average values than the PLA tests, on both dimensions, and also presented similar measurements in tests 2 and 3.

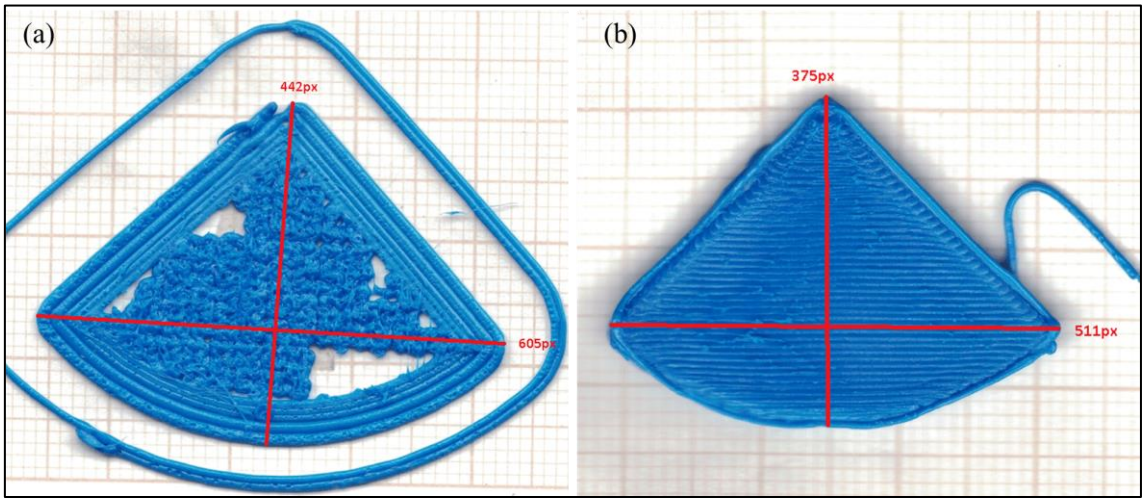

Figure 4. Workpiece dimensions. (a) 6ºth PLA test, (b) 5ºth PLA test

3.2 Superficial anomalies

Regarding the results obtained from the superficial anomalies assessment, each printed workpiece is presented in figure format. In each figure, yellow dashed circles and ellipses indicate the regions evaluated in the workpiece in order to facilitate visualization.

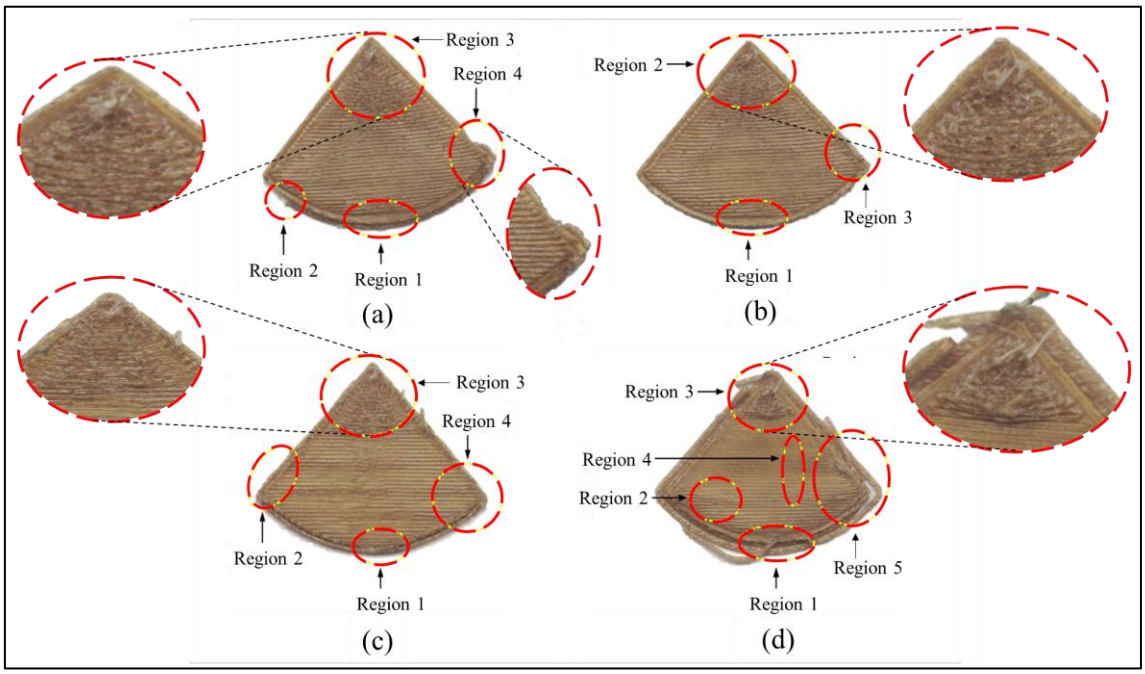

Figure 5. PETG workpieces. (a) Test 1, (b) Test 2, (c) Test 3, (d) Test 4

Initially, as can be observed in the workpieces presented in Figure 5, all tests performed with PETG showed very similar defect regions. As an example of the similarity of the defect regions, one may look at the upper part of the workpieces, as seen in Region 3 in Figure 5 (a), Figure 5 (c) and Figure 5 (d), and Region 2 in Figure 5 (b). There is no apparent cause or easy to spot printing parameter responsible for the appearance of such anomaly, but the hypothesis that has been developed is that there was an accumulation of filament deposited in these regions.

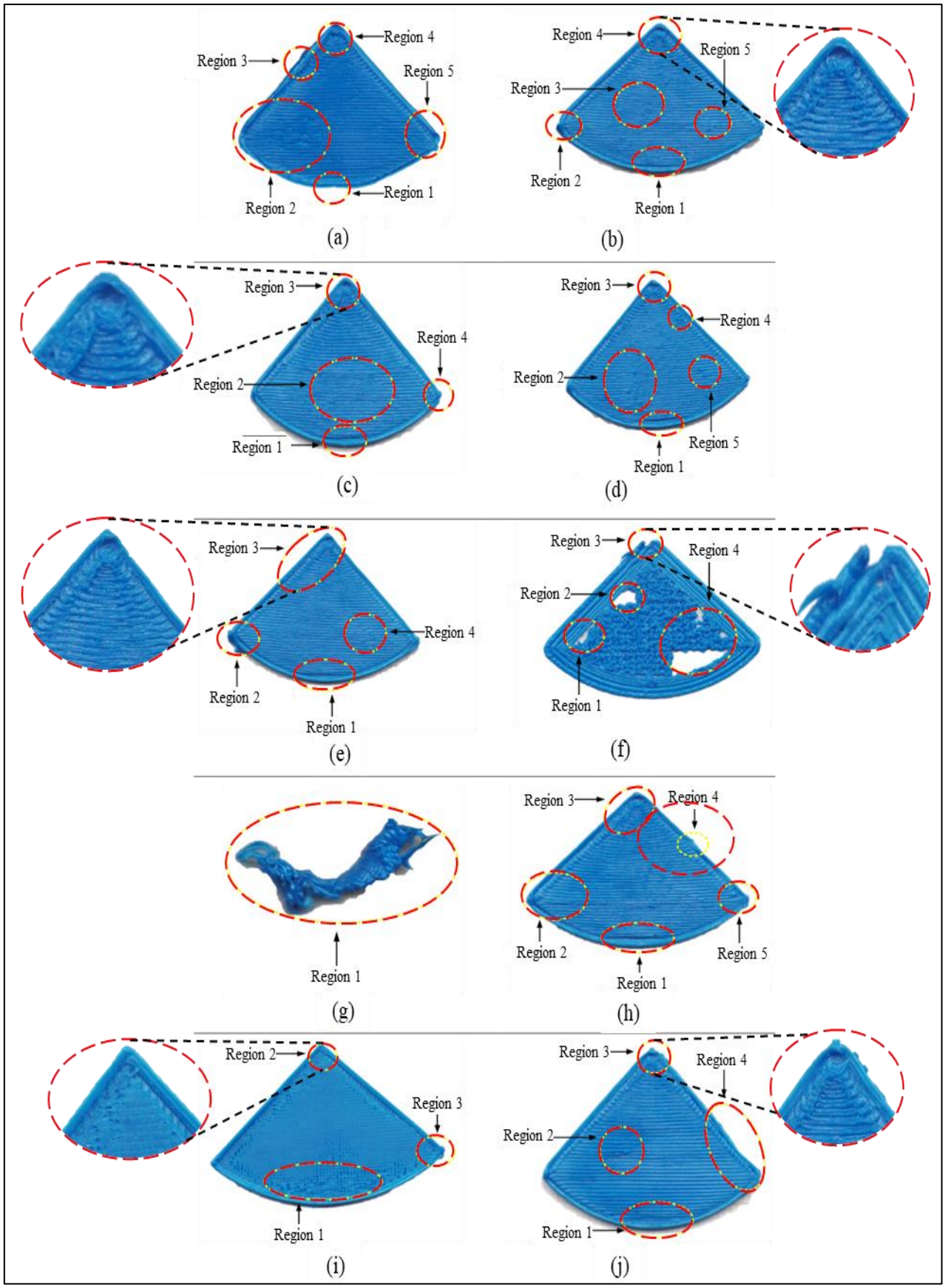

Figure 6. PLA workpieces. (a) Test 1, (b) Test 2, (c) Test 3, (d) Test 4, (e) Test 5, (f) Test 6, (g) Test 7, (h) Test 8, (i) Test 9, (j) Test 10

Furthermore, Region 4 of Figure 5 (a) highlights a geometric defect in one of the part's curves. Such deformation does not occur in the same way in the other tests, which possibly indicates the printing speed of the first layer as the printing parameter producing the defect. On the other hand, Region 1, in all workpieces presented on Figure 5, presents a deformation that can be attributed to the chosen infill pattern, considering the geometry of the part, and regardless of the printing material used, as it is possible to observe it also on the workpieces presented in Figure 6. In order to conclude that defective Region 1 is the result of a wrong choice of the infill pattern, one can look at the 6ºth PLA test in Figure 6 (f), which does not present the same defect in its Hilbert Curve filling pattern.

The 7ºth PLA test, represented in Figure 6 (g), suffered a random error during printing, which caused a complete deformation of its geometry. Another punctual anomaly that can be observed in most PLA printed workpieces is the deformation that occurs at the top corner, where the start and end points of the printing of the contour lines are likely to be found. As it is present in the majority of tests in Figure 6, one hypothesis to explain the occurrence of this defect is that the extruder nozzle was positioned too close to the table, flattening the workpieces at this position.

4. CONCLUSION

The digitalization of the surfaces of the parts printed in PLA filament and PETG filament allowed the evaluation of dimensional variations and the occurrence of surface anomalies caused by the selection of different printing parameters in the slicing stage of the FFF process. Through visual inspection of the digitized parts, it was possible to observe that the selection of certain printing parameters influenced the dimensions of the obtained parts, with some parts presenting higher dimensional values than those originally defined for the proposed 3D model. It was also observed in this study that through the inspection of the digitized parts it was possible to identify punctual defects in different regions of the parts.

Finally, it can be concluded that with the use of visual inspection method to investigate the digitized surface of monolayer parts obtained by the FFF process, it is possible to determine the occurrence of dimensional variations and surface anomalies arising from an incorrect definition of parameters during the slicing step, assisting the operator of the FFF process in decision making regarding the parameters of printing being adopted for a given process. Moreover, it should be noted that the approach performed in this work is initial and additional studies are necessary in order to validate the proposed method under different slicing and printing conditions.

5. ACKNOWLEDGMENTS

This work was supported by the São Paulo Research Foundation (FAPESP) (grants #2016/22038-8 and #2019/22788-5) and by the National Council for Scientific and Technological Development (CNPq) (grants #306435/2017-9)

6. REFERENCES

Boschetto, A.; Bottini, L. *Roughness prediction in coupled operations of fused deposition modeling and barrel finishing*. Journal of Materials Processing Technology, [*s. l.*], v. 219, p. 181–192, 2015.

Carmo, M.G.F. *et al.* Study of the Defects and Geometric Anomalies on Monolayer Parts Obtained by Fused Deposition Modeling Process. Proceedings, Online, v. 69, n. 1, p. 40, 2020.

Da Silva, J.V.L. *Process Planning for Rapid Prototyping* (in Portuguese). *In*: VOLPATO, Neri (org.). Prototipagem Rápida - Tecnologias e Aplicações. 1. ed. São Paulo: Blucher, 2007. p. 37.

Dawoud, M.; Taha, I.; Ebeid, S.J. *Mechanical behaviour of ABS: An experimental study using FDM and injection moulding techniques*. Journal of Manufacturing Processes, [*s. l.*], v. 21, p. 39–45, 2016.

Ge, C. *et al. Towards automatic visual inspection: A weakly supervised learning method for industrial applicable object detection*. Computers in Industry, [*s. l.*], v. 121, 2020.

ISO/ASTM. *ISO/ASTM 52900: Additive manufacturing - General principles - Terminology*. International Standard, [*s. l.*], v. 5, p. 1–26, 2015.

Kocisko, M. *et al. Postprocess Options for Home 3D Printers*. Procedia Engineering, [*s. l.*], v. 196, n. June, p. 1065–1071, 2017.

Liu, Z. *et al. A critical review of fused deposition modeling 3D printing technology in manufacturing polylactic acid parts*. [*S. l.: s. n.*], 2019.

Liu, Z.; Lei, Q.; Xing, S. *Mechanical characteristics of wood, ceramic, metal and carbon fiber-based PLA composites fabricated by FDM*. Journal of Materials Research and Technology, [*s. l.*], v. 8, n. 5, p. 3743–3753, 2019.

Lopes, T.G. *et al. The First Layer as Quality Indicator of the Planning of the 3D Printing Process* (in Portuguese). *In*: , 2020, Bauru. Anais do XXVII Simpósio de Engenharia de Produção (SIMPEP). Bauru: [*s. n.*], 2020. p. 1–12.

Lopes, T.G. *et al. The Use of Additive Manufacturing in Research Projects* (in Portuguese). *In*: , 2018, Lins-SP. (Anderson Pazin & Fábio Lúcio Meira, Org.) Anais do II Congresso de Inovação e Tecnologia – FATEC Lins. Lins-SP: Centro Paula Souza, 2018. p. 104–112.

Nakajima, R. *et al. A study on the effect of defect shape on defect detection in visual inspection*. Procedia Manufacturing, [*s. l.*], v. 39, n. 2019, p. 1641–1648, 2019.

Oettmeier, K.; Hofmann, E. *Additive manufacturing technology adoption: an empirical analysis of general and supply chain-related determinants*. Journal of Business Economics, [*s. l.*], 2017.

Rodríguez-Panes, A.; Claver, J.; Camacho, A.M. *The influence of manufacturing parameters on the mechanical behaviour of PLA and ABS pieces manufactured by FDM: A comparative analysis*. Materials, [*s. l.*], v. 11, n. 8, 2018.

Santana, L. *et al. Comparative Study Between PETG and PLA for 3D Printing Through Thermal, Chemical and Mechanical Characterization* (in Portuguese). Matéria (Rio de Janeiro), [*s. l.*], 2018.

Sculpteo. *the state of 3D PRINTING EDITION 2018*. [*s. l.*], p. 23, 2020.

Singh, S.; Ramakrishna, S.; Singh, R. *Material issues in additive manufacturing: A review*. Journal of Manufacturing Processes, [*s. l.*], v. 25, p. 185–200, 2017.

Voelker, M.M. *Quantitative surface inspection methods for metal castings*. Dissertation. 121 f. 2016. - Iowa State University, Digital Repository, Ames, 2016.

Volpato, N. *Additive Manufacturing: 3D Printing Technologies and Applications* (in Portuguese). 1. ed. São Paulo: Blucher, 2017.

Wendt, C. *et al. Processing and Quality Evaluation of Additive Manufacturing Monolayer Specimens*. Advances in Materials Science and Engineering, [*s. l.*], v. 2016, p. 1–8, 2016.

Wu, H.; Yu, Z.; Wang, Y. *Experimental study of the process failure diagnosis in additive manufacturing based on acoustic emission*. Measurement, [*s. l.*], v. 136, p. 445–453, 2019.

Wu, Y. *et al. Process Monitoring of Fused Deposition Modeling through Profile Control*. *In*: , 2019. 2018 IEEE International Conference on Cyborg and Bionic Systems, CBS 2018. [*S. l.: s. n.*], 2019.

Zhang, S. *et al. Visual inspection of steel surface defects based on domain adaptation and adaptive convolutional neural network*. Mechanical Systems and Signal Processing, [*s. l.*], v. 153, 2021.

7. RESPONSIBILITY NOTICE

The authors are the only responsible for the printed material included in this paper.